



Single-cell RNA sequencing for characterizing the immune communication and iron metabolism roles in CD31⁺ glioma cells

Yiming Guan¹, Yu Luan², Shanshan Zhao², Meiyang Li³, Francesco Girolamo⁴, Joshua D. Palmer⁵, Qi Guan²

¹Department of Surgery and Cancer, Imperial College London, London, UK; ²Clinical Laboratory Center, The First People's Hospital of Shenyang (Shenyang Brain Hospital), Shenyang Medical College, Shenyang, China; ³Tuberculosis Laboratory, Shenyang Tenth People's Hospital (Shenyang Chest Hospital), Shenyang, China; ⁴Department of Translational Biomedicine and Neuroscience (DiBrain), University of Bari Aldo Moro, Bari, Italy; ⁵Department of Radiation Oncology, Ohio State University, Columbus, OH, USA

Contributions: (I) Conception and design: Y Guan, Q Guan; (II) Administrative support: Y Luan, S Zhao, M Li; (III) Provision of study materials or patients: S Zhao, Y Guan; (IV) Collection and assembly of data: M Li, Y Guan; (V) Data analysis and interpretation: Y Guan; (VI) Manuscript writing: All authors; (VII) Final approval of manuscript: All authors.

Correspondence to: Qi Guan, PhD. Clinical Laboratory Center, The First People's Hospital of Shenyang (Shenyang Brain Hospital), Shenyang Medical College, 67 Qingquan Road, Shenyang 110041, China. Email: guanqi1231@sina.com.

Background: Gliomas are aggressive brain tumors marked by complex cellular interactions and significant immune cell infiltration. This study investigated the role of CD31⁺ immune cells, specifically macrophages and T cells, in the glioma microenvironment through single-cell RNA sequencing (scRNA-seq).

Methods: We employed the CellChat framework to map cell-cell communication pathways and used Monocle3 for pseudotime trajectory analysis to characterize the signaling and developmental progressions within CD31⁺ cells. Pathways such as osteopontin (SPP1) and major histocompatibility complex class II (MHC-II) were analyzed in terms of their role in immune regulation, and we examined the expression of ferritin, an iron-binding protein, to assess its potential function in modulating CD31⁺ cell activity.

Results: Our findings highlight the expression of key pathways, including SPP1 and MHC-II, influencing immune regulation. Ferritin was found to be highly expressed in CD31⁺ cells, suggesting a dual role in iron metabolism and immune modulation within the glioma microenvironment.

Conclusions: This study clarified the distinct roles of CD31⁺ immune cells in glioma progression and identified ferritin as a potential therapeutic target for modulating immune responses in gliomas. These findings may offer new directions in glioma research and the development of immunotherapy, which can aid in improving treatment outcomes.

Keywords: CD31; glioma; ferritin; immune regulation; tumor microenvironment

Submitted Feb 19, 2025. Accepted for publication Apr 08, 2025. Published online Apr 25, 2025.

doi: 10.21037/tcr-2025-377

View this article at: <https://dx.doi.org/10.21037/tcr-2025-377>

Introduction

Gliomas are the most common and aggressive form of brain tumor, accounting for a significant proportion of deaths due to central nervous system malignancies (1). Despite extensive research efforts, gliomas remain difficult to manage, with high recurrence rates and poor survival outcomes (2). Gliomas can be classified into different types based on their molecular and genetic characteristics,

including the presence or absence of mutations in the isocitrate dehydrogenase (*IDH*) gene, which is used to distinguish between *IDH*-mutant and *IDH*-wildtype gliomas (3-5). These tumors also differ in their cellular composition, histopathological features, and prognosis, leading to substantial heterogeneity within glioma subtypes. Understanding the mechanisms of tumor progression, immune infiltration, and resistance to therapies is essential

for improving treatment outcomes. However, much remains unknown about the molecular and cellular underpinnings of gliomas, particularly in the context of the tumor microenvironment and its interaction with immune cells (6). Further research is critical to identifying novel therapeutic targets and biomarkers that could improve the management of patients with glioma.

A promising area of glioma research involves the role of immune cells within the tumor microenvironment. In particular, CD31, also known as platelet endothelial cell adhesion molecule-1 (PECAM-1), has traditionally been considered a marker for endothelial cells and is well recognized for its role in angiogenesis and maintaining vascular integrity (7). However, recent studies have demonstrated that CD31 is also expressed by certain immune cells, including macrophages and T cells, within the tumor microenvironment (8,9). These CD31⁺ immune cells exhibit functional differences from their CD31⁻ counterparts (10). For instance, CD31⁺ macrophages and T cells have been associated with altered immune responses, including the modulation of inflammation and immune tolerance, suggesting a distinct role for CD31 in the immune landscape of gliomas. The presence of

CD31 on these immune cells may influence their ability to infiltrate tumor tissues, engage in cell-cell communication, and contribute to the immunosuppressive environment often seen in aggressive gliomas (11). Despite the growing body of evidence supporting the role of CD31 in immune cell function, the specific characteristics and functional relevance of CD31⁺ immune cells in glioma remain poorly understood. Further investigation into the role of CD31-expressing immune cells within gliomas could provide novel insights into novel immune-regulatory mechanisms and potential therapeutic avenues.

Single-cell RNA sequencing (scRNA-seq) has emerged as a powerful tool for investigating the cellular heterogeneity of tumors at unprecedented resolution. This next-generation sequencing (NGS) technology allows for the transcriptional profiling of individual cells, enabling researchers to explore the gene expression patterns of distinct cell types within a tissue sample (12,13). In the context of glioma, scRNA-seq provides an opportunity to dissect the complex cellular architecture of the tumor microenvironment, identify key cell populations, and study their interactions at a molecular level (14,15). By isolating and analyzing individual cells, researchers can distinguish between cancerous and noncancerous cells and explore the diverse populations of immune and stromal cells that contribute to tumor progression. The ability to map out the cellular landscape of gliomas with such detail holds promise for discovering new biomarkers, therapeutic targets, and mechanisms of resistance to treatment. Moreover, scRNA-seq facilitates the study of rare cell populations that may play critical roles in tumor evolution but are otherwise difficult to characterize using bulk RNA-sequencing approaches (16).

In this study, we used scRNA-seq technology to clarify the role of CD31⁺ immune cells, particularly macrophages and T cells, in gliomas. By analyzing a dataset of CD31⁺ cells from glioma samples, we sought to characterize their transcriptional profiles and distinct characteristics compared to CD31⁻ immune cells. Using two complementary techniques—cell-cell communication analysis with the CellChat framework and pseudotime trajectory analysis with Monocle3—we investigated the functional relevance of these cells. The cell-cell communication analysis revealed key pathways involved in immune regulation and tumor progression through the mapping of signaling interactions within the tumor microenvironment, while pseudotime analysis traced the developmental trajectories of CD31⁺ immune cells, providing a dynamic view of their behavior.

Highlight box

Key findings

- CD31⁺ immune cells, including macrophages and T cells, play pivotal roles in glioma progression, with distinct functions revealed through single-cell RNA sequencing (scRNA-seq).
- Ferritin, an iron-binding protein, was identified as a key regulator of CD31⁺ cell activity, linking iron metabolism to immune modulation in gliomas.
- Mural cells, despite their low abundance, exhibited a high interaction rate with other cell types, underscoring their significance in the glioma microenvironment.

What is known and what is new?

- The involvement of immune cells, particularly macrophages and T cells, in the glioma microenvironment has been established.
- This study is the first to highlight the role of CD31⁺ immune cells and mural cells in glioma using scRNA-seq data. It identified ferritin as a potential therapeutic target for immune modulation.

What is the implication, and what should change now?

- Targeting ferritin and the identified ligand-receptor interactions, such as osteopontin-CD44 interaction, offers new therapeutic avenues to modulate the glioma microenvironment.
- Increased focus should be paid to the role of mural cells and their interactions, which could lead to novel strategies for disrupting tumor progression and enhancing immunotherapy outcomes.

Our findings demonstrated that CD31⁺ macrophages and T cells exhibit unique communication patterns and functional profiles, with ferritin, a key iron-binding protein, emerging as a critical regulator of these cells' activity and function. The enriched expression of ferritin in CD31⁺ cells suggests a link between iron metabolism and immune function within the tumor microenvironment. This study highlights the potential of ferritin as a therapeutic target, offering new avenues for research and immunotherapies aimed at modulating the immune landscape in gliomas to improve outcomes. We present this article in accordance with the MDAR reporting checklist (available at <https://tcr.amegroups.com/article/view/10.21037/tcr-2025-377/rc>).

Methods

Data acquisition and preprocessing

We downloaded the scRNA-seq data of four brain glioblastoma samples from the Gene Expression Omnibus platform, with the tumor core selected as the region of interest. The data suppliers subjected single-cell suspensions, enriched for CD31⁺ cells using magnetic-activated cell sorting (MACS), to scRNA-seq using a 10× genomics-based single-cell protocol. The dataset downloaded was from the Gene Expression Omnibus (accession No. GSE162631) (17). The raw sequence reads were analyzed by Cell Ranger v3.0.1 under the default parameters. This study was conducted in accordance with the Declaration of Helsinki and its subsequent amendments.

Single-cell analysis

The scRNA-seq data were analyzed using the Seurat package (version 4.3.0.1) to process and visualize the dataset (18). We first merged the four individual cell files to create a single Seurat object. This object was normalized using the `NormalizeData` function, followed by the identification of highly variable genes with the `FindVariableFeatures` function. Next, principal component analysis (PCA) was performed using the `RunPCA` function to reduce dimensionality. A Uniform Manifold Approximation and Projection (UMAP) was then applied for visualization via the `RunUMAP` function based on the first 15 principal components. Clustering of cells was performed with the `FindNeighbors` and `FindClusters` functions, with a resolution of 0.2. The clustering results were visualized using UMAP plots.

Pseudotime analysis with Monocle3

Pseudotime trajectory analysis was conducted using Monocle3 to infer the developmental progression of cells (19,20). The Seurat UMAP coordinates were transferred to Monocle3 using UMAPPlot. We constructed a cell dataset using the expression matrix and metadata from Seurat. After the data were normalized, dimensionality reduction was performed using Monocle3's `reduce_dimension` function, and cells were clustered using the `cluster_cells` function with a resolution of 1×10^{-7} . A cell trajectory graph was learned using the `learn_graph` function, and cells were ordered along the pseudotime trajectory. Genes of interest were plotted across the pseudotime to visualize their expression trends along the differentiation pathways.

Cell-cell communication analysis with CellChat

Cell-cell communication was examined using the CellChat package, which analyzed the ligand-receptor interactions between cell types (21). The `createCellChat` function was used to create the CellChat object from the Seurat data, after which `identifyOverExpressedGenes` and `identifyOverExpressedInteractions` were applied to determine the overexpressed ligand-receptor pairs (L-R pairs). The probability of interactions between cell subtypes was computed using the `computeCommunProb` function. Network plots were generated to visualize the interaction strength and frequency between different cell populations. Pathway-specific analyses were conducted for key signaling pathways.

Statistical analysis

All statistical analyses conducted in this study were generated with R software version 4.3.1 (The R Foundation for Statistical Computing, Vienna, Austria). A P value <0.05 was considered to be statistically significant.

Results

scRNA transcriptional profiling of CD31⁺ cells in glioblastoma brain samples

In order to explore the cell-cell communication pattern within glioblastoma, we used the scRNA data from the GSE162631 dataset. We selected four glioblastoma samples enriched for CD31⁺ cells through MACS. *Table 1* summarizes the patient information from the four samples.

Table 1 Clinical information of patients included in this study

Parameters	Patient			
	1	2	3	4
Histology	GBM	GBM	GBM	GBM
Gender	Female	Female	Male	Male
Age (years)	58	54	63	52
Recurrence	Primary	Primary	Primary	Primary
<i>IDH</i> status	Wild-type	Wild-type	Wild-type	Wild-type
1p/19q status	Non-codel	Non-codel	Non-codel	Non-codel
Location	Right parietal lobe	Left temporal lobe	Right occipital lobe	Right frontal lobe
GFAP	+	+	+	+
OLIG2	+	+	+	+
NF	+	–	+	+
Ki67	20%+	20%+	25%+	15%+
p53	+	+	–	+
MMP9	+	–	–	–
S100	+	+	+	+
Vimentin	+	+	+	+
Syn	+	–	–	+
MBP	NA	–	+	–
ATRX	+	+	–	+
EMA	+	+	+	+
MGMT	–	+	+	–
NeuN	–	–	–	–
LCA	NA	–	–	–
EGFR	+	NA	NA	NA

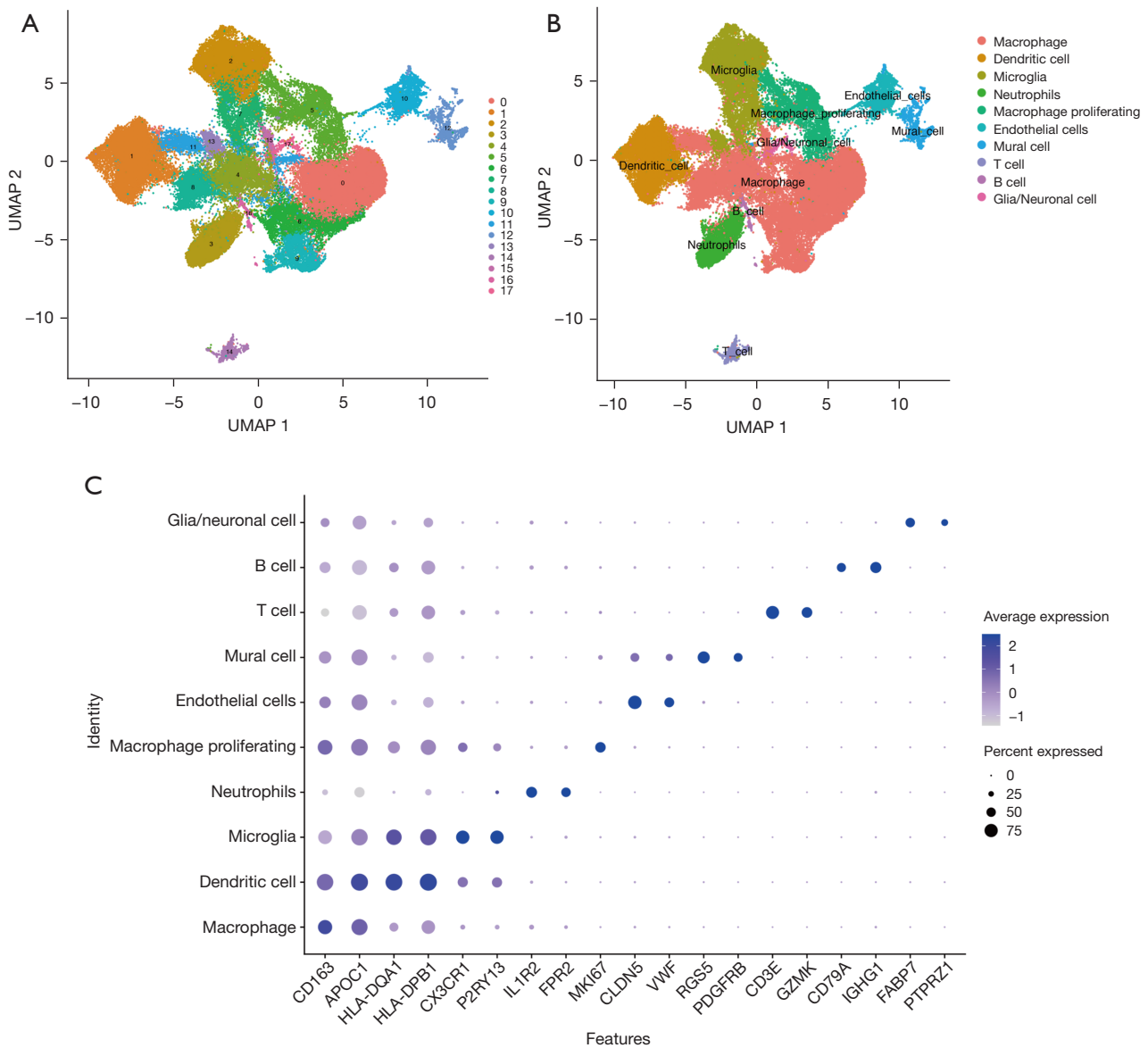
+, present of the marker; –, absent of the marker. GBM, glioblastoma; *IDH*, isocitrate dehydrogenase; NA, not available.

Our single-cell analysis identified 18 distinct clusters (Figure 1A). Based on the cell markers provided by the data contributors, these clusters were classified into 10 cell types, including macrophages, dendritic cells, microglia, neutrophils, proliferating macrophages, endothelial cells, mural cells, T cells, B cells, and glia/neuronal cells (Figure 1B). Nineteen gene markers used for this classification were visualized through a dot plot (Figure 1C).

Pseudotime analysis of glioblastoma samples identified key genes

To explore the development of the dataset, we used Monocle3 to construct a pseudotime model of all cell

clusters within the dataset, which was demonstrated in UMAP plots (Figure 2A,2B). In addition to visualizing the overall structure of the dataset, we identified specific genes of interest across the developmental trajectory (Figure 2C). Notably, *CD2*, *CD3D*, *CD3E*, and *CD3G*, key markers of T cells, were variably expressed along the pseudotime axis, reflecting the involvement of immune-related pathways in tumor progression. Furthermore, we observed interesting expression patterns of ferroptosis-related genes, such as *FTH1* and *FTL*, being highly expressed in the neutrophil's population and the macrophage cluster that sat in the middle, suggesting a potential link between ferroptosis and tumor biology, particularly within endothelial cell populations. The expression of these genes aligns with the



pseudotime trajectory, suggesting their role in glioblastoma progression. Additionally, markers such as *SELE* and *TRBC2* were also expressed along the trajectory, providing further insights into immune and endothelial interactions within the tumor microenvironment. This analysis highlights the dynamic changes in gene expression across the pseudotime trajectory, underscoring the potential roles of ferroptosis and immune modulation in glioblastoma development.

High intercellular communication among CD31⁺ cells revealed by CellChat

In order to explore the cellular interaction within the CD31⁺ cells of the dataset, we used CellChat, a bioinformatics tool designed especially for the exploration of cell-cell communication via a ligand-receptor method. By analyzing both number of interactions and interaction

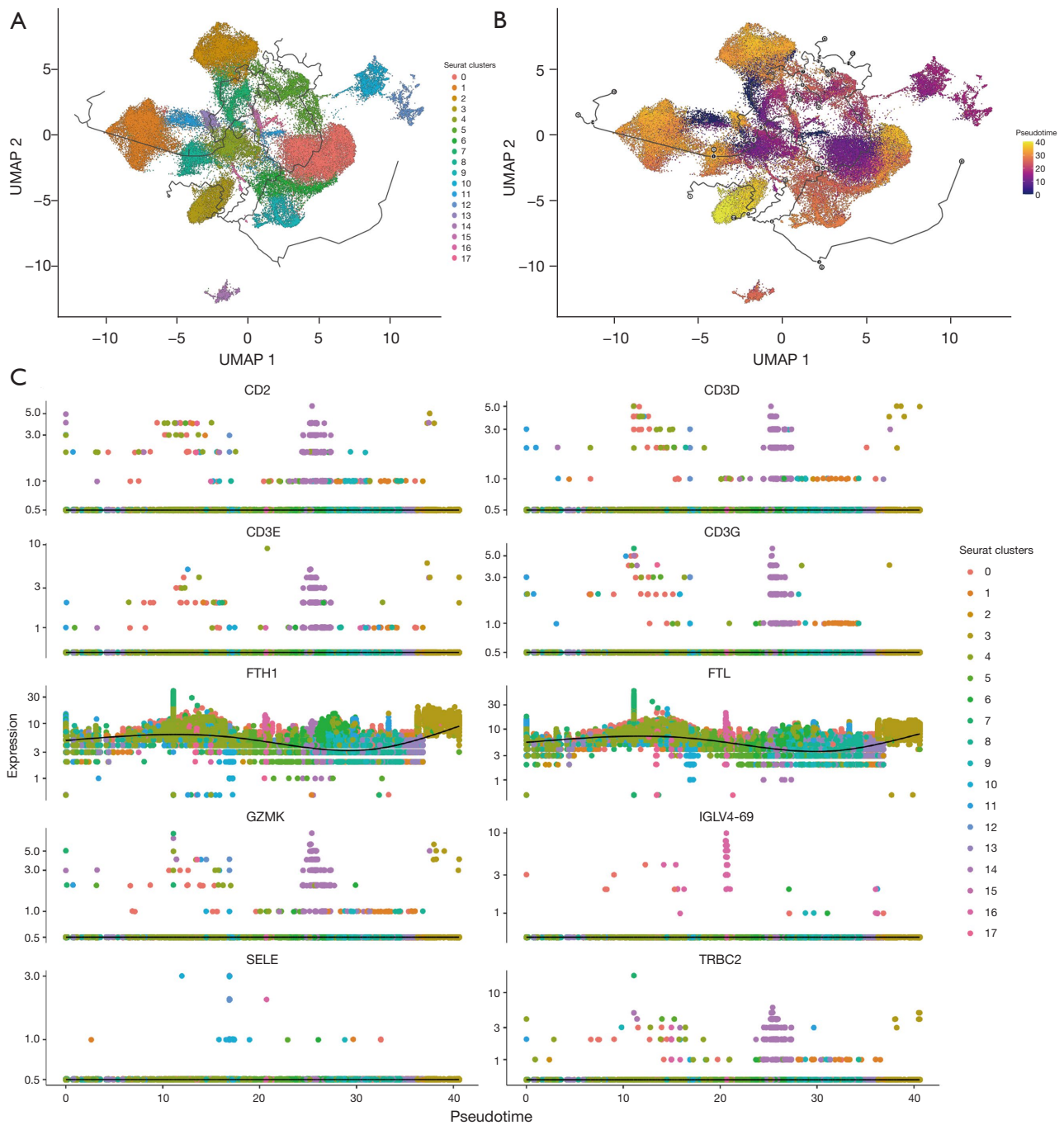


Figure 2 Trajectory analysis depicting the heterogeneity of CD31⁺ glioma cells. (A) Pseudotime and trajectory analysis via Monocle3 with coloring according to cluster. (B) Pseudotime and trajectory analysis via Monocle3 with coloring according to pseudotime. (C) Dot plots demonstrating genes that varied the most in this trajectory. A Moran's index value greater than 0 indicates a positive spatial correlation. UMAP, Uniform Manifold Approximation and Projection.

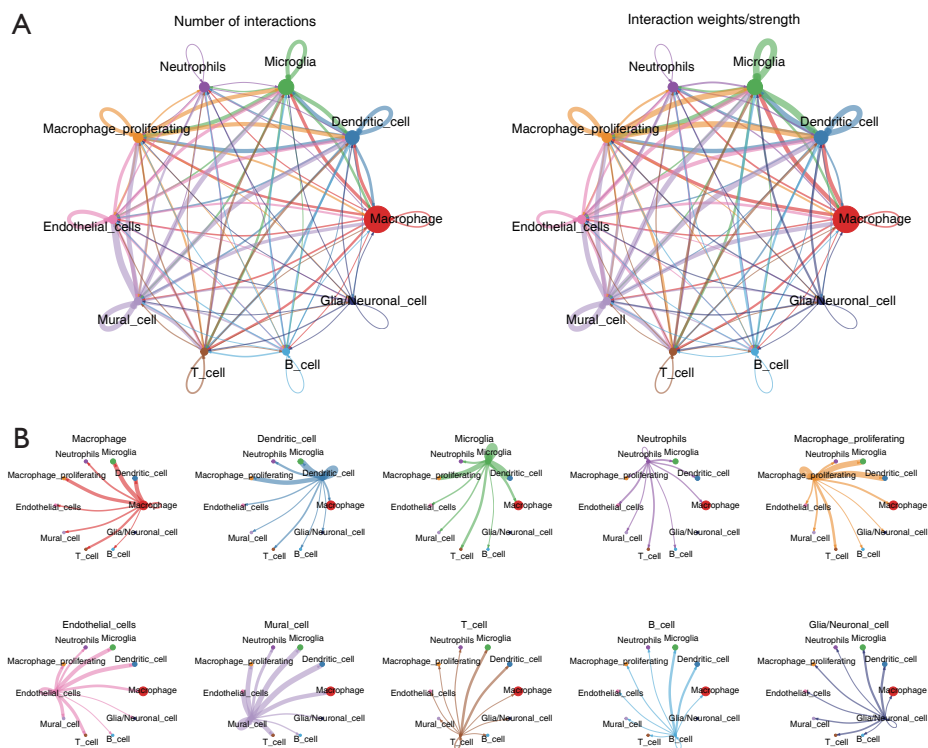


Figure 3 Interaction dynamics and intercellular communication networks of CD31⁺ cells. (A) The plots of the number of interactions and interaction weight/strength for CD31⁺ cells. Thicker lines indicate a higher number of interactions and greater intensity of communication between cell types. (B) Intercellular plots for each cell type between all cell types. The thickness of the lines reflects the strength of interactions between the respective cell types.

weight/strength, we discovered a high interaction rate among all cell types (Figure 3A). Cell types such as microglia also displayed a high tendency of self-interaction. Although the relative cell number was not high, mural cells within the dataset appeared to interact heavily with myeloid cell types, including macrophages and dendritic cells. We then separated the interactions to show how each cell type interacted with other cell types, creating a clearer picture of the interactive status of each cell type (Figure 3B). We found that although the number of mural cells was negligible compared to the number of macrophages, the interaction number and strength of mural cells and other cell types was larger than that of macrophages. These results prompted us to reconsider the role that mural cells play in the tumor microenvironment of glioma.

Identifying the key single signaling pathway networks within CD31⁺ glioma

To characterize the ligand-receptor interaction in single

signaling pathways, we programmed the circle plot to display the intercellular communication separated by single signaling pathways. The top four key signaling pathways were identified and displayed within the circle plots (Figure 4A). Apart from the osteopontin (SPP1) signaling pathway, for which the interactions were pervasive within the dataset, signaling pathways such as collagen and fibronectin 1 (FN1) appeared to be more dependent on mural cells. The major histocompatibility complex class II (MHC-II) pathway depended more on myeloid cells such as macrophages and dendritic cells. We then visualized the interaction status in heatmaps, which supported the key role of this pathway (Figure 4B). In order to clarify the role each cell type in a single signaling pathway, we generated a heatmap classifying cells into sender, receiver, mediator, and influencer of the given signaling pathway (Figure 4C). In line with our assumptions, macrophages were the sender of the SPP1 signaling pathway, and microglia assumed multiple roles as receiver, mediator, and influencer. The collagen pathway seemed to be important only in mural cells, while

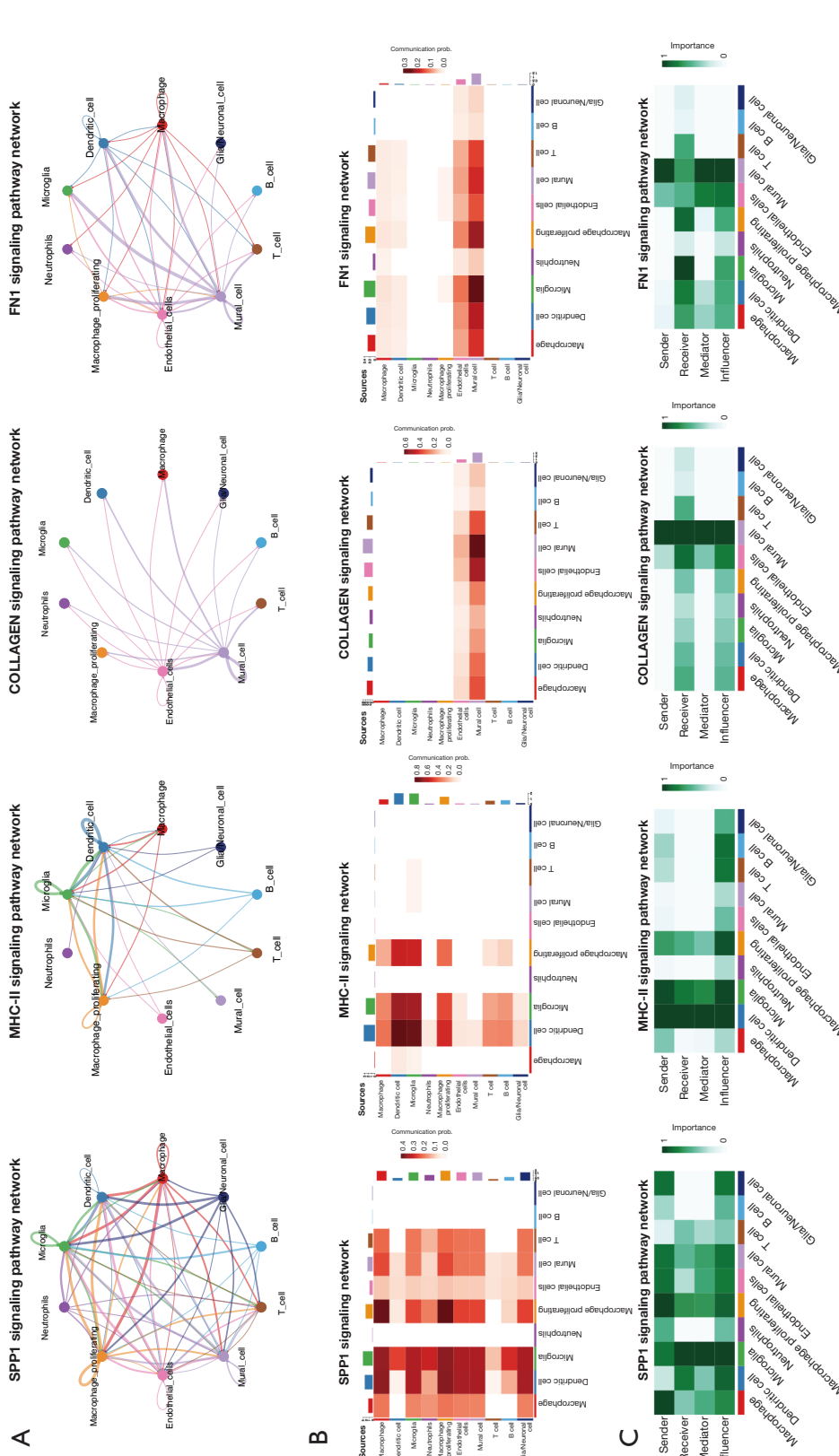


Figure 4 Intercellular communication networks and relative importance of cell groups in CD31⁺ cells across the top four most significant signaling pathways. (A) Circle plots representing the intercellular communication networks within CD31⁺ cell populations for the top four signaling pathways (SPP1, MHC-II, collagen, and FN1). A thicker line indicates a higher number of interactions and stronger interaction strength between cell types. (B) Heatmaps displaying the communication probabilities of the top four signaling pathways. The communication probability for each signaling pathway was computed by summarizing the probabilities of its associated L-R pairs. A darker color indicates a higher probability of communication between cell types. The total probability of communication between the selected and other cell types are demonstrated on the X- and Y-axis. (C) Heatmaps showing the relative importance of each cell group based on computed network centrality measures, which assess the roles of each cell type as sender, receiver, mediator, or influencer. A darker color represents a greater importance in the respective networks. FN1, fibronectin 1; L-R pairs, ligand-receptor pairs; MHC-II, major histocompatibility complex class II; Prob., probability; SPP1, osteopontin.

within the FN1 signaling pathway, microglia assumed the receiver role, with mural cells assuming the other roles. Dendritic cells occupied all four roles within the MHC-II signaling pathway, while microglia played both the role of sender and influencer, while proliferating macrophages were influencers. Analysis of single signaling pathways revealed key pathways within the dataset, while emphasizing the key role of certain cells within a given pathway.

Crucial L-R pairs identified within the key signaling pathways

We then attempted to determine which L-R pairs function within the key signaling pathways. By comparing the relative contribution of each L-R pair, we were able to identify the key L-R pairs (*Figure 5A*). The SPP1 ligand interacted with integrin subunit alpha V (ITGAV) + integrin subunit beta 1 (ITGB1) the most, followed by CD44. Within the MHC-II pathway, the HLA-DRA-CD4 L-R pair contributed to the intercellular interaction more than other L-R pairs. The collagen pathway contained two highly common L-R pairs, namely COL4A1-CD44 and COL4A2-CD44. The FN1 ligand paired with both CD44 and ITGAV + ITGB1. The expression of each ligand or receptor gene within different cell types is displayed in *Figure 5B*. SPP1 was found to be expressed in every cell type within the CD31⁺ dataset. The genes of the collagen pathway, however, displayed a tendency to be expressed mainly in mural cells. Similar results were found for the *FN1* gene, except that in addition to mural cells, endothelial cells were also found to express FN1. Taking the L-R pairs' relative contribution into consideration, it is clear that these certain L-R pairs exerted considerable influence within the tumor microenvironment of glioma.

Reclassification of the T-cell populations revealed key L-R pairs of CD8⁺ T cells

To obtain a more in-depth understanding of the T-cell population within the CD31⁺ glioma dataset, we conducted reclassification of the T cell population, enabling us to obtain six subpopulations, namely CD8⁺ T cells, CD4⁺ T cells, cycling T cells, natural killer (NK) cells, monocytes, and macrophages (*Figure 6A*). The genes that were most differentially expressed, or the marker genes, were visualized within a heatmap (*Figure 6B*). We first explored the interaction number and weight/strength among every subpopulation of T cells (*Figure 6C*). We found that

although the number of cells of each subpopulation varied, with CD8⁺ T cells constituting the highest proportion, the interaction among each cell type displayed similar intensity. This result was then confirmed by the separation each cell type to display the interaction between one cell type and all other cell types (*Figure 6D*). By comparing the strength and importance of each signaling pathway, we identified the centrality of the C-C motif chemokine ligand (CCL) signaling pathway within the subpopulations of T cells (*Figure 6E*). High interaction intensity was found between CD8⁺ T cells and macrophages. Through comparison, we identified the highest contributing L-R pair, the CCL5-CCR1 pair. The interaction of the CCL5-CCR1 L-R pair among all T-cell subpopulations is presented in *Figure 6F*, and its relative contribution with other L-R pairs in the CCL signaling pathway is presented in *Figure 6G*. To increase the comprehensiveness of our L-R pair study, we explored all key L-R pairs within CellChat and generated a thorough dot plot consisting of every highly communicated L-R pair between CD8⁺ T cells and other T-cell subpopulations (*Figure 6H*). We discovered that the SPP1-CD44 L-R pair had the greatest communication probability between CD8⁺ T cells and macrophages. As the SPP1-CD44 pair is often implicated in promoting tumor progression by fostering an immunosuppressive environment and supporting macrophage polarization toward a tumor-promoting (M2-like) phenotype. This could reduce the effectiveness of CD8⁺ T cell-mediated anti-tumor immunity. The result suggested that the SPP1-CD44 L-R pairs could play a key role in the intercellular communication between CD8⁺ T cells and macrophages within the CD31⁺ glioma dataset.

Key L-R pairs of M2 macrophages identified via myeloid-cell reclassification

We then continued our exploration by conducting reclassification of the myeloid cell population, which enabled us to obtain 10 subpopulations, namely fibroblast, neutrophil-like (neu-like) myeloid cells, monocytes, M1 macrophages, M2 macrophages, cycling macrophages, proliferating macrophages, microglia, dendritic cells, and neutrophils (*Figure 7A*). The marker genes of each subpopulation were demonstrated within a heatmap (*Figure 7B*). We clarified interaction number and weight/strength among every subpopulation of myeloid cells (*Figure 7C*). We found differences in the interaction intensity between each of the cell types. This was confirmed

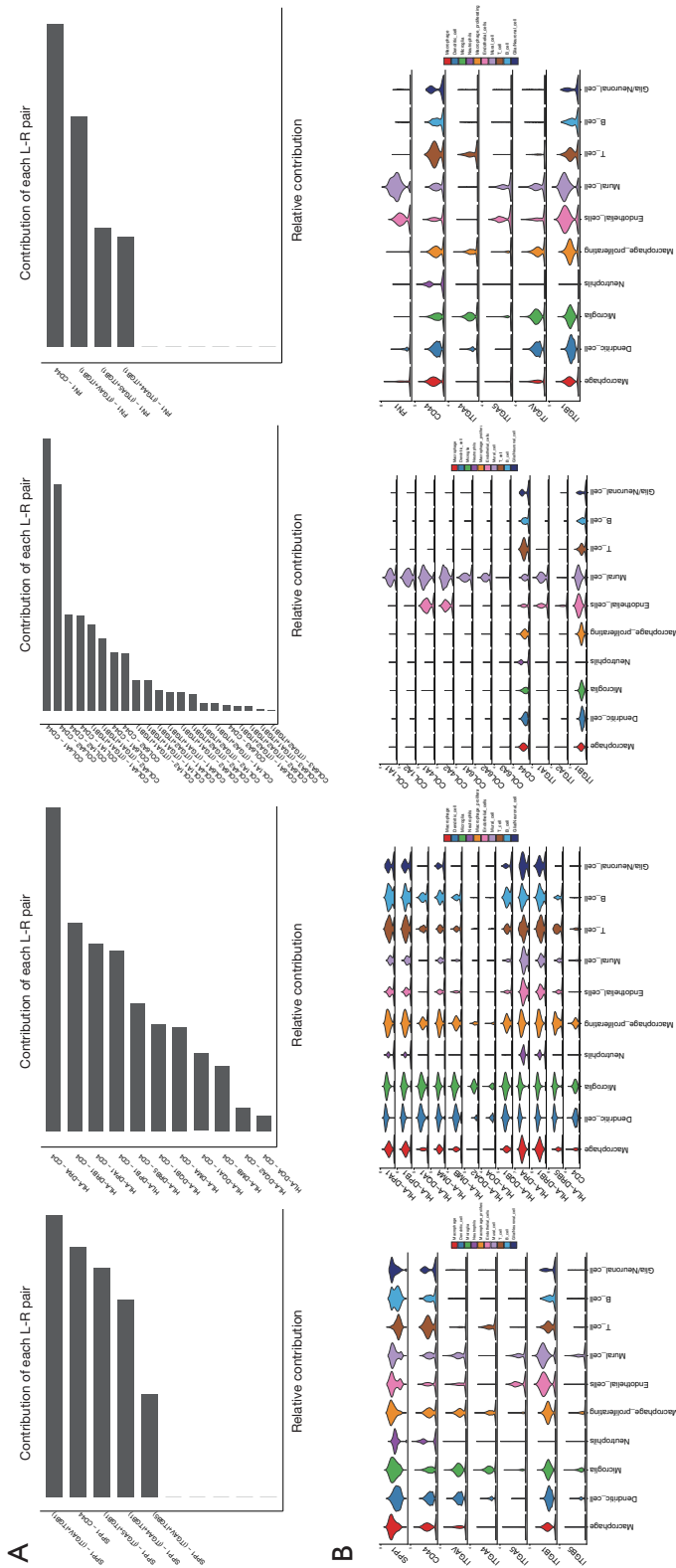


Figure 5 Relative contribution of each L-R pair to the overall communication network of signaling pathways and the expression patterns of signaling genes involved in the inferred signaling network. (A) Relative contribution of each L-R pair to the overall communication network of signaling pathways, represented as the ratio of the total communication probability of the inferred network of each L-R pair to that of the signaling pathways. (B) Violin plots showing the expression patterns of signaling genes involved in the inferred signaling network. Normalized expression levels are shown in the violin plots. L-R pair, ligand-receptor pair.

of 6 clusters based on the average log₂ fold change. (C) Plots for the number of interactions and interaction weight/strength of the T-cell clusters. The thicker the line is, the higher the number of interactions and the stronger the interaction weight/strength between the two cell types. (D) Intercellular plots for each T-cell subtype between all T-cell subtypes. The thicker the line is, the stronger the interaction weight/strength between the two cell types. (E) Plot of the interaction weight/strength of the CCL signaling pathway network [similar to (C)]. (F) Plot of the interaction weight/strength of the CCL5-CCR1 L-R pair [similar to (C)]. (G) Relative contribution of each L-R pair to the overall communication network of the CCL signaling pathway, which is the ratio of the total communication probability of the inferred network of each L-R pair to that of the signaling pathways. (H) Dot plot depicting all significant L-R pairs between CD8⁺ T cells and other T-cell subpopulations. The color of the dots represents the communication probability, and the dot size reflects the computed P values computed from a one-sided permutation test. CCL, C-C motif chemokine ligand; Commun. Prob., communication probability; L-R pair, ligand-receptor pair; NK, natural killer; UMAP, Uniform Manifold Approximation and Projection.

by the separation of each cell type to display the interaction between one cell type and all other cell types (*Figure 7D*). The interaction between microglia and M2 macrophages was stronger than that between any two other cell types. We determined the viability of the CCL signaling pathway in myeloid cell subsets by comparing the strength and importance of each signaling pathway (*Figure 7E*). By comparison, we identified the L-R pair with the highest contribution, CCL5-CCR1. *Figure 7F* shows the interaction of the CCL5-CCR1 L-R pair in all myeloid cell subsets, and *Figure 7G* shows the comparison with the contribution of other L-R pairs of the CCL signaling pathway. To improve the comprehensiveness of L-R pair studies, we identified all the significant L-R pairs in CellChat and generated a complete dot plot containing each highly communicative L-R pair between M2 macrophages and other myeloid cell subsets (*Figure 7H*). We discovered that the SPP1-CD44 L-R pair demonstrated the highest communication probability between M2 macrophages and neu-like myeloid cells, M2 and M1 macrophages, and M2 macrophages and dendritic cells. Considering that the SPP1-CD44 L-R pair was identified to be central within CD8⁺ T cells, this L-R pair has the potential to be a key regulating checkpoint, controlling the interaction of multiple intercellular communications within the glioma microenvironment.

Discussion

CD31 has been long regarded as a marker for endothelial cells, and its expression can be used to identify endothelial cells. However, previous studies have reported that CD31 can appear on the surface of many other cell types, especially immune cells (8,9). The expression of CD31 on T cells and macrophages has been proven to be an indicator of altered behavior as compared to that of non-expressing macrophages. Moreover, recent research identified that the

increase in the abundance of circulating CD31⁺ T cells is a potential mechanism by which exercise reduces the risk of cardiovascular disease (22). In another study, the scRNA-seq data of CD31⁺ cells within glioma was acquired to create a molecular atlas of human brain endothelial cells, revealing the heterogeneity of the blood-brain barrier and its changes in glioma (17). Five distinct endothelial cell phenotypes were identified, each representing a different state of activation and impairment of the blood-brain barrier and linked to various tumor-related locations. However, this study focused mostly on the endothelial cell population, with no emphasis on other cell types that could be potential influencers of the microenvironment. Therefore, in our study, we used this set of data to examine the behavior of CD31⁺ immune cells, with special focus on the T-cell and macrophage population. We discovered that CD31 expression is universal across multiple cell subpopulations, and the CD31⁺ populations appeared to display enhanced immune activity. Pseudotime analysis revealed the key role that ferritin plays within the CD31⁺ cell population. Cell-cell communication analysis revealed the strong interaction strength between different CD31⁺ cell types and identified key ligand-receptor pathways directing the interaction. This study was based on the scRNA-seq data of CD31⁺ glioma cells, predicts the functional dynamics of these CD31⁺ immune cell types.

Gliomas are characterized by its unique microenvironment. Due to the hindering of the blood-brain barrier, the infiltration of peripheral immune cells, such as T cells, into the brain is restricted (23). This phenomenon has been observed in previous scRNA-seq analyses of glioma (17). In our study, the majority of the CD31⁺ cells were classified as myeloid cells. This can also be partly attributed to the fact that glioma involves the recruitment and reprogramming of myeloid cells, such as macrophages and microglia, to support tumor growth (24). These tumor-associated

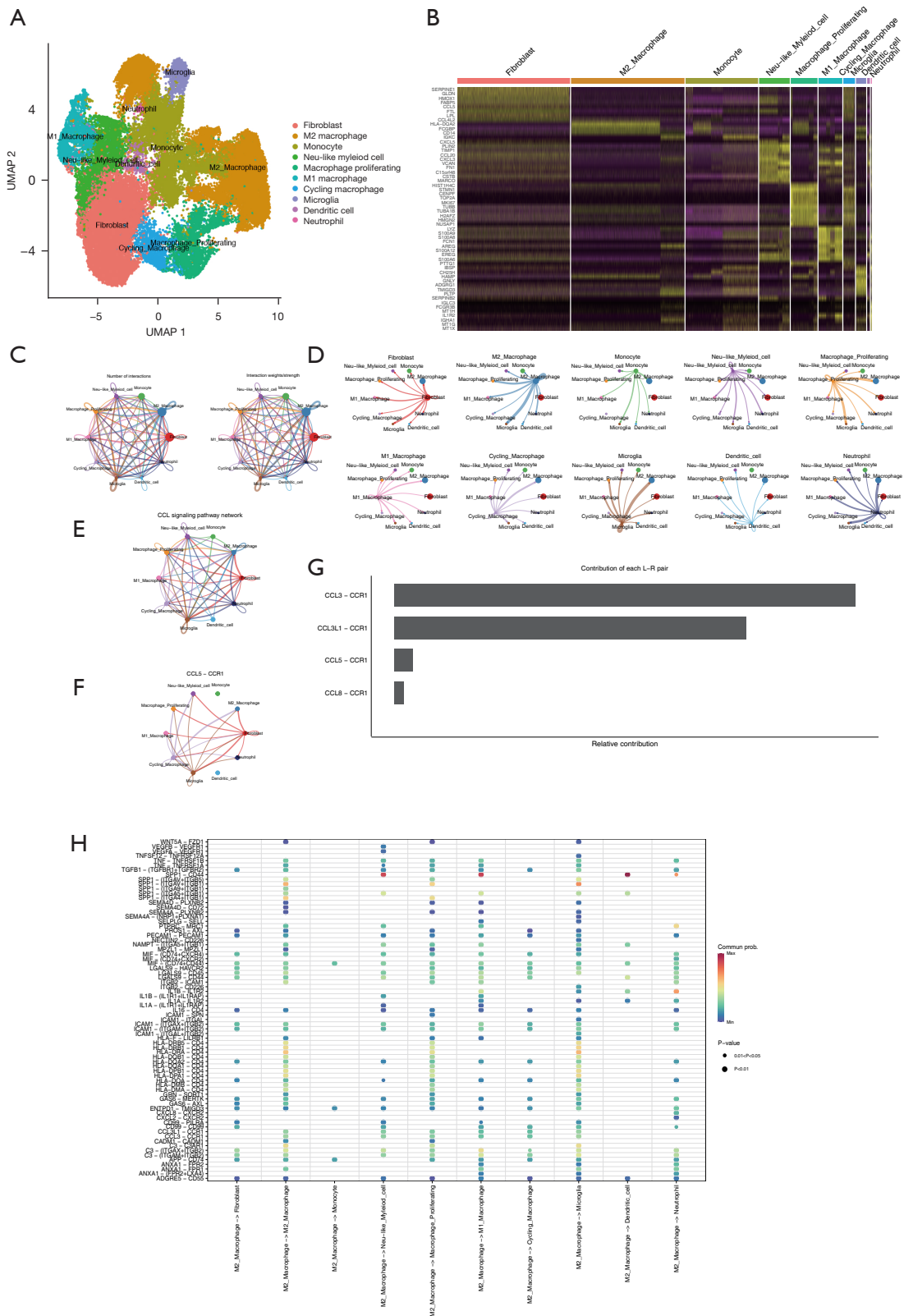


Figure 7 The landscape and cell-cell communication network of the myeloid cell population in CD31⁺ cells of the glioma cohort. (A) UMAP plot demonstrating how the myeloid cell population was classified into 10 subpopulations. (B) Heatmap showing the differential

gene expression of 10 clusters based on the average log₂ fold change. (C) Plots of the number of interactions and the interaction weight/strength of the myeloid cell clusters. The thicker the line is, the higher the number of interactions and the stronger the interaction weight/strength between the two cell types. (D) Intercellular plots for each myeloid cell subtype between all myeloid cell subtypes. The thicker the line is, the stronger the interaction weight/strength between the two cell types. (E) Plot of the interaction weight/strength of the CCL signaling pathway network [similar to (C)]. (F) Plot of the interaction weight/strength of the CCL5-CCR1 L-R pair [similar to (C)]. (G) Relative contribution of each L-R pair to the overall communication network of the CCL signaling pathway, which is the ratio of the total communication probability of the inferred network of each L-R pair to that of signaling pathways. (H) Dot plot depicting all significant L-R pairs between M2 macrophages and other myeloid cell subpopulations. The color of the dots represents the communication probability, and the dot size reflects the computed P values computed from a one-sided permutation test. CCL, C-C motif chemokine ligand; Commun. Prob., communication probability; L-R pair, ligand-receptor pair; neu-like, neutrophil-like; UMAP, Uniform Manifold Approximation and Projection.

macrophages (TAMs) and microglia form a significant portion of the glioma microenvironment and often display immunosuppressive phenotypes (25). This allows the tumor to evade immune surveillance and promotes a tumorigenic environment. In our study, macrophages constituted the largest cell population. The macrophages with marker of proliferation Ki-67 (MKI67) positivity were classified as proliferating macrophages and separate from the main macrophage cell population. The abundance of myeloid cells allows for further classification of this population.

Pseudotime analysis has been applied in single-cell analysis to identify the more primitive and more advanced cell type (26). This is conducted by constructing a “fake” model from which the cell type is derived in an evolutionarily manner. In this study, we constructed a pseudotime model of all the CD31⁺ cells in the glioma dataset. The trajectory model of the 18 cell clusters was constructed, and the pseudotime origin of the clusters was tracked to the macrophage population. This result supports the fact that the proliferating macrophage population and other myeloid cells were more evolutionarily advanced. In addition, we identified genes that varied the most along the trajectory and plotted the top 10 genes. Cellular markers of T cells were identified within the top genes. Genes that reflect the immune status were also identified. Notably, *FTH1* and *FTL*, two genes that encode ferritin, were identified as varying along the trajectory. Ferritin regulates iron storage and protects against oxidative stress by sequestering free iron (27). In tumors, ferritin is involved in iron metabolism, angiogenesis, and protecting cells from ferroptosis—a form of iron-dependent cell death (28). Ferritin is also overexpressed in glioma, with recent studies demonstrating that its elevated levels correlate with higher tumor grades, enhanced angiogenesis, resistance to ferroptosis, and poorer overall survival (28,29). Ferritin

genes *FTH1* and *FTL* has been identified as overexpressing in glioma by previous studies (30-32). In the context of gliomas, ferritin's involvement in regulating ferroptosis may provide insights into how these tumors resist certain types of cell death, particularly in highly oxidative environments such as the brain (29). The upregulation of ferritin may act as a protective mechanism for immune cells within the tumor, allowing them to maintain function in iron-rich, oxidative environments. These findings support the diagnostic efficacy of ferritin as a biomarker and its potential as a prognostic indicator. Additionally, the strong connection between iron metabolism and immune function points to ferritin as a potential therapeutic target. Moreover, ferritin appears to modulate the tumor microenvironment by influencing iron homeostasis, thereby impacting immune cell activity. Increased ferritin levels have been linked to a greater infiltration of TAMs—particularly M2-like, immunosuppressive subtypes—and regulatory T cells, which further contributes to an immunosuppressive milieu that promotes tumor progression (33). Ferritin can also act as a nano vector for the delivery of drugs to glioma (33). By modulating ferritin levels, we may be able to influence immune cell activity and enhance the efficacy of immunotherapy strategies.

Cell-cell communication analysis of scRNA data is built upon the expression of certain L-R pairs (21). The interaction weights, or strengths, among different cell types are constructed based on the total expression amount of ligand genes and receptor genes. In this study, we conducted a thorough intercellular ligand-receptor interaction analysis on the CD31⁺ cells in the glioma dataset. We first checked the interaction of each cell type with all other cell types. Unexpectedly, although they had a lower abundance, mural cells appeared to have the greatest degree of interaction with other cell types. However, this

cell type has not been extensively studied in relation to CD31⁺. Mural cells are contractile cells that surround blood vessels, including pericytes and smooth muscle cells (34). They support vascular stability, regulate blood flow, and maintain the blood-brain barrier. These cells play key roles in angiogenesis and vessel maturation and are involved in various diseases such as cancer and cardiovascular conditions (35,36). Blocking certain pathways of mural cells can impact the angiogenesis of glioma (37). Our study further discovered that mural cells may play a more active role in glioma progression than has been previously thought.

CellChat can identify the highly interactive signaling pathways within the dataset. We used this function within our study and discovered four signaling pathway networks of high intensity. The four pathways were SPP1, MHC-II, collagen, and FN1. SPP1 is involved in immune regulation, cell survival, and tissue remodeling via binding to integrins and CD44 to mediate cellular adhesion and migration (38,39). In this study, we identified its function within macrophages, including proliferating macrophages. MHC-II molecules present extracellular antigen-derived peptides to CD4⁺ T cells, initiating adaptive immune responses and playing a critical role in immune system function (40). The dendritic cell population displayed high intensity on the MHC-II signaling pathway. Collagen is a structural protein that provides tensile strength and support to tissues, and its signaling pathways influence cellular adhesion, migration, and differentiation during tissue development and repair (41). It was only identified in the mural cell population within this study. FN1 is a glycoprotein involved in cell adhesion, migration, and wound healing, acting through integrins to mediate cellular interactions with the extracellular matrix and influence cell signaling pathways related to growth and survival (42). A high intensity of interaction was discovered between the mural cell and microglia population. We then further explored the individual L-R pairs within the selected signaling pathways and, to our knowledge, are the first to discover that CD44 interacts with SPP1, collagen, and FN1. CD44 is a transmembrane glycoprotein that functions as a cell surface receptor involved in a variety of cellular processes, including cell adhesion, migration, and signaling (43). It primarily binds to hyaluronic acid, a component of the extracellular matrix, but also interacts with other ligands such as SPP1, collagen, and FN1 (44). Moreover, CD44 was found to be expressed in all cell populations. Key ligands such as SPP1, collagen type I alpha 1 (COL1A1), and FN1 all bind to CD44. A previous study identified SPP1⁺ macrophages as

prognostic indicators of glioma (45). Although SPP1 was also universally expressed on all cell types, the expression of COL1A1 and FN1 was limited, with mural cells expressing both ligands, and endothelial cells expressing only FN1. Our study suggests CD44 as a central mediator within the identified signaling networks, particularly in facilitating cellular interactions across diverse cell types. Considering that mural cells demonstrated significant involvement in the FN1 and collagen signaling pathways, which are critical for extracellular matrix remodeling and angiogenesis—given their extensive interactions with macrophages and microglia—mural cells may contribute to the immunosuppressive and tumorigenic environment in gliomas by facilitating communication between immune and vascular cells. These findings call for a reevaluation of the roles that mural cells play in glioma biology, particularly in their ability to influence immune cell function and tumor angiogenesis.

Among all cell types included in this study, T cells were the most extensively researched cell population. The subclustering for T cells includes well-known cell types such as CD8⁺ T cells, or cytotoxic T cells, in addition to CD4⁺ T cells, or helper T cells (46). Cycling T cells were another T cell subpopulation. Cycling T cells actively proliferate during immune responses when they encounter antigens, such as those from pathogens or cancer cells (47). Their rapid proliferation generates effector T cells to combat infections or tumors. Subclustering of T cells in our study identified six types: CD8⁺ T cells, CD4⁺ T cells, cycling T cells, NK cells, and two types with myeloid characteristics. The CD8⁺ population was predominant, but there was low CD8A expression, likely due to the nonactivated state of these cells. Previous research has suggested that CD31 expression is absent in acutely activated CD8⁺ T cells, which may explain this observation (48). In contrast, markers for cycling T cells, such as *MKI67*, *TOP2A*, and *HMGB2*, were highly expressed, in line with the proliferative nature of these cells. Cell-cell communication analysis revealed strong interactions between CD8⁺ T cells and monocytes, particularly through CD8-HLA L-R pairs, highlighting the significance of antigen presentation in glioma immune responses.

According to previous research, CD31 expression is the most prevalent among the myeloid cell population. In this study, a considerable number of cells were classified into the myeloid population. A reclustering was conducted to the myeloid cells that were initially classified into macrophages, dendritic cells, microglia, and proliferating

macrophages. This reclustering attributed these myeloid cells into 10 clusters, with eight of them having a myeloid origin, including M1 and M2 macrophages, monocytes, microglia, dendritic cells, proliferating and cycling macrophages, and neu-like myeloid cells. Monocytes are circulating immune cells that migrate to tissues and differentiate into macrophages or dendritic cells, playing a key role in immune surveillance and inflammation (49). M1 macrophages are proinflammatory macrophages that eliminate pathogens and secrete cytokines to drive immune responses (50). M2 macrophages are anti-inflammatory macrophages involved in tissue repair and immune regulation. Proliferating macrophages expand locally during immune responses, and cycling macrophages contribute to tissue regeneration (51). Microglia are resident macrophages in the central nervous system that maintain brain homeostasis and respond to injury or infection (52). Dendritic cells are antigen-presenting cells that activate T cells by capturing and presenting antigens, linking innate and adaptive immunity (53). Neu-like myeloid cells mimic neutrophils in their rapid response to infection, primarily by engulfing pathogens and releasing antimicrobial factors (54). We also conducted cell-cell communication analysis of the myeloid population and found that the anti-inflammatory M2 macrophages were the most active. This might suggest an immunosuppressive environment within glioma. In the case of L-R pairs, we also observed a high intensity of interaction between SPP1 and CD44, with SPP1 mainly expressing on M2 macrophages. This could also suggest the key role of M2 macrophages within the immunosuppressive environment. This reclustering study identified the elevated activity of M2 macrophages within the glioma tumor microenvironment.

By elucidating the dual role of ferritin in regulating iron metabolism and immune modulation, our study opens promising avenues for novel therapeutic strategies and improved prognostic evaluation in glioma. Specifically, targeting ferritin or its related pathways (such as the SPP1-CD44 axis) could disrupt the immunosuppressive tumor microenvironment and sensitize glioma cells to existing therapies. Moreover, our application of scRNA-seq has been instrumental in uncovering the intricate cellular heterogeneity within glioma, revealing distinct immune subpopulations and dynamic cell-cell interactions that would be masked in bulk analyses. While this technology provides unprecedented resolution in characterizing tumor ecosystems, challenges such as data integration, interpretation of sparse datasets, and the

underrepresentation of rare cell types remain. Addressing these challenges will be critical for translating our findings into effective, personalized treatment approaches for glioma patients.

However, there are several limitations to our dataset and analysis. Our results were based on a single dataset. In addition, in a study focusing on CD31⁺ cells, we did not have access to a matching CD31⁻ cell population for comparison due to the limitations introduced by the data provider; moreover, no *in vitro* experiment was conducted to validate our results. Avenues of further research could include additional datasets, the analysis of cell populations without CD31 expression as a control group, and basic experiments to validate the results.

Conclusions

Our study analyzed the behavior and communication of CD31⁺ cells in glioma using scRNA-seq data. We identified 18 distinct cell clusters, including immune cells such as T cells and macrophages, highlighting the complexity of the tumor microenvironment. Pseudotime analysis suggested a role for ferritin in iron regulation and angiogenesis within glioma. Furthermore, key ligand-receptor interactions, such as SPP1-CD44 interaction, were identified in the communication between T cells, macrophages, and mural cells, underscoring their significance in immune regulation and tissue remodeling. Notably, mural cells exhibited a higher interaction rate despite their lower abundance, indicating their crucial role in the tumor microenvironment. Our findings revealed the role of CD31⁺ cells in glioma, highlighting their impact on immune and vascular responses and providing a strong foundation for further research.

Acknowledgments

None.

Footnote

Reporting Checklist: The authors have completed the MDAR reporting checklist. Available at <https://tcr.amegroups.com/article/view/10.21037/tcr-2025-377/rc>

Peer Review File: Available at <https://tcr.amegroups.com/article/view/10.21037/tcr-2025-377/prf>

Funding: This work was supported by grants from the

Sub-Project of Key project of the National Key R&D Program “Basic Scientific Research Conditions and Major Scientific Instruments and Equipment R&D” (No. 2022YFF0710300).

Conflicts of Interest: All authors have completed the ICMJE uniform disclosure form (available at <https://tcr.amegroups.com/article/view/10.21037/tcr-2025-377/prf>). The authors have no conflicts of interest to declare.

Ethical Statement: The authors are accountable for all aspects of the work in ensuring that questions related to the accuracy or integrity of any part of the work are appropriately investigated and resolved. This study was conducted in accordance with the Declaration of Helsinki and its subsequent amendments.

Open Access Statement: This is an Open Access article distributed in accordance with the Creative Commons Attribution-NonCommercial-NoDerivs 4.0 International License (CC BY-NC-ND 4.0), which permits the non-commercial replication and distribution of the article with the strict proviso that no changes or edits are made and the original work is properly cited (including links to both the formal publication through the relevant DOI and the license). See: <https://creativecommons.org/licenses/by-nc-nd/4.0/>.

References

1. Miller KD, Ostrom QT, Kruchko C, et al. Brain and other central nervous system tumor statistics, 2021. *CA Cancer J Clin* 2021;71:381-406.
2. Omuro A, DeAngelis LM. Glioblastoma and other malignant gliomas: a clinical review. *JAMA* 2013;310:1842-50.
3. Chen R, Smith-Cohn M, Cohen AL, et al. Glioma Subclassifications and Their Clinical Significance. *Neurotherapeutics* 2017;14:284-97.
4. Miller JJ. Targeting IDH-Mutant Glioma. *Neurotherapeutics* 2022;19:1724-32.
5. Board WCoTE. World Health Organization Classification of Tumours of the Central Nervous System. Lyon: International Agency for Research on Cancer; 2021.
6. Barthel L, Hadamitzky M, Dammann P, et al. Glioma: molecular signature and crossroads with tumor microenvironment. *Cancer Metastasis Rev* 2022;41:53-75.
7. Lertkiatmongkol P, Liao D, Mei H, et al. Endothelial functions of platelet/endothelial cell adhesion molecule-1 (CD31). *Curr Opin Hematol* 2016;23:253-9.
8. Marelli-Berg FM, Clement M, Mauro C, et al. An immunologist's guide to CD31 function in T-cells. *J Cell Sci* 2013;126:2343-52.
9. McKenney JK, Weiss SW, Folpe AL. CD31 expression in intratumoral macrophages: a potential diagnostic pitfall. *Am J Surg Pathol* 2001;25:1167-73.
10. Kohler S, Thiel A. Life after the thymus: CD31+ and CD31- human naive CD4+ T-cell subsets. *Blood* 2009;113:769-74.
11. Lutzky VP, Carnevale RP, Alvarez MJ, et al. Platelet-endothelial cell adhesion molecule-1 (CD31) recycles and induces cell growth inhibition on human tumor cell lines. *J Cell Biochem* 2006;98:1334-50.
12. Slovin S, Carissimo A, Panariello F, et al. Single-Cell RNA Sequencing Analysis: A Step-by-Step Overview. *Methods Mol Biol* 2021;2284:343-65.
13. Zhang Y, Wang D, Peng M, et al. Single-cell RNA sequencing in cancer research. *J Exp Clin Cancer Res* 2021;40:81.
14. Darmanis S, Sloan SA, Croote D, et al. Single-Cell RNA-Seq Analysis of Infiltrating Neoplastic Cells at the Migrating Front of Human Glioblastoma. *Cell Rep* 2017;21:1399-410.
15. Eisenbarth D, Wang YA. Glioblastoma heterogeneity at single cell resolution. *Oncogene* 2023;42:2155-65.
16. Hwang B, Lee JH, Bang D. Single-cell RNA sequencing technologies and bioinformatics pipelines. *Exp Mol Med* 2018;50:1-14.
17. Xie Y, He L, Lugano R, et al. Key molecular alterations in endothelial cells in human glioblastoma uncovered through single-cell RNA sequencing. *JCI Insight* 2021;6:e150861.
18. Hao Y, Hao S, Andersen-Nissen E, et al. Integrated analysis of multimodal single-cell data. *Cell* 2021;184:3573-3587.e29.
19. Trapnell C, Cacchiarelli D, Grimsby J, et al. The dynamics and regulators of cell fate decisions are revealed by pseudotemporal ordering of single cells. *Nat Biotechnol* 2014;32:381-6.
20. Cao J, Spielmann M, Qiu X, et al. The single-cell transcriptional landscape of mammalian organogenesis. *Nature* 2019;566:496-502.
21. Jin S, Guerrero-Juarez CF, Zhang L, et al. Inference and analysis of cell-cell communication using CellChat. *Nat Commun* 2021;12:1088.
22. Baker CJ, Min D, Marsh-Wakefield F, et al. Circulating CD31(+) Angiogenic T cells are reduced in prediabetes and increase with exercise training. *J Diabetes Complications*

- 2024;38:108868.
23. van Tellingen O, Yetkin-Arik B, de Gooijer MC, et al. Overcoming the blood-brain tumor barrier for effective glioblastoma treatment. *Drug Resist Updat* 2015;19:1-12.
 24. Ding AS, Routkevitch D, Jackson C, et al. Targeting Myeloid Cells in Combination Treatments for Glioma and Other Tumors. *Front Immunol* 2019;10:1715.
 25. Khan F, Pang L, Dunterman M, et al. Macrophages and microglia in glioblastoma: heterogeneity, plasticity, and therapy. *J Clin Invest* 2023;133:e163446.
 26. Qiu X, Mao Q, Tang Y, et al. Reversed graph embedding resolves complex single-cell trajectories. *Nat Methods* 2017;14:979-82.
 27. Knovich MA, Storey JA, Coffman LG, et al. Ferritin for the clinician. *Blood Rev* 2009;23:95-104.
 28. Shesh BP, Connor JR. A novel view of ferritin in cancer. *Biochim Biophys Acta Rev Cancer* 2023;1878:188917.
 29. Hou W, Xie Y, Song X, et al. Autophagy promotes ferroptosis by degradation of ferritin. *Autophagy* 2016;12:1425-8.
 30. Gong H, Gao M, Lin Y, et al. TUG1/MAZ/FTH1 Axis Attenuates the Antiglioma Effect of Dihydroartemisinin by Inhibiting Ferroptosis. *Oxid Med Cell Longev* 2022;2022:7843863.
 31. Liu J, Gao L, Zhan N, et al. Hypoxia induced ferritin light chain (FTL) promoted epithelia mesenchymal transition and chemoresistance of glioma. *J Exp Clin Cancer Res* 2020;39:137.
 32. Li H, Yang C, Wei Y, et al. Ferritin light chain promotes the reprogramming of glioma immune microenvironment and facilitates glioma progression. *Theranostics* 2023;13:3794-813.
 33. Marrocco F, Falvo E, Mosca L, et al. Nose-to-brain selective drug delivery to glioma via ferritin-based nanovectors reduces tumor growth and improves survival rate. *Cell Death Dis* 2024;15:262.
 34. Siekmann AF. Biology of vascular mural cells. *Development* 2023;150:dev200271.
 35. Crouch EE, Bhaduri A, Andrews MG, et al. Ensembles of endothelial and mural cells promote angiogenesis in prenatal human brain. *Cell* 2022;185:3753-3769.e18.
 36. Lin A, Peiris NJ, Dhaliwal H, et al. Mural Cells: Potential Therapeutic Targets to Bridge Cardiovascular Disease and Neurodegeneration. *Cells* 2021;10:593.
 37. Merk L, Regel K, Eckhardt H, et al. Blocking TGF- β - and Epithelial-to-Mesenchymal Transition (EMT)-mediated activation of vessel-associated mural cells in glioblastoma impacts tumor angiogenesis. *Free Neuropathol* 2024;5:4.
 38. Icer MA, Gezmen-Karadag M. The multiple functions and mechanisms of osteopontin. *Clin Biochem* 2018;59:17-24.
 39. Kumari A, Kashyap D, Garg VK. Osteopontin in cancer. *Adv Clin Chem* 2024;118:87-110.
 40. Axelrod ML, Cook RS, Johnson DB, et al. Biological Consequences of MHC-II Expression by Tumor Cells in Cancer. *Clin Cancer Res* 2019;25:2392-402.
 41. Su H, Karin M. Collagen architecture and signaling orchestrate cancer development. *Trends Cancer* 2023;9:764-73.
 42. Dalton CJ, Lemmon CA. Fibronectin: Molecular Structure, Fibrillar Structure and Mechanochemical Signaling. *Cells* 2021;10:2443.
 43. Hassn Mesrati M, Syafruddin SE, Mohtar MA, et al. CD44: A Multifunctional Mediator of Cancer Progression. *Biomolecules* 2021;11:1850.
 44. Mattheolabakis G, Milane L, Singh A, et al. Hyaluronic acid targeting of CD44 for cancer therapy: from receptor biology to nanomedicine. *J Drug Target* 2015;23:605-18.
 45. Tang W, Lo CWS, Ma W, et al. Revealing the role of SPP1(+) macrophages in glioma prognosis and therapeutic targeting by investigating tumor-associated macrophage landscape in grade 2 and 3 gliomas. *Cell Biosci* 2024;14:37.
 46. Zheng L, Qin S, Si W, et al. Pan-cancer single-cell landscape of tumor-infiltrating T cells. *Science* 2021;374:abe6474.
 47. Liu S, Huang Z, Fan R, et al. Cycling and activated CD8(+) T lymphocytes and their association with disease severity in influenza patients. *BMC Immunol* 2022;23:40.
 48. Newman DK, Fu G, McOlash L, et al. Frontline Science: PECAM-1 (CD31) expression in naïve and memory, but not acutely activated, CD8⁺ T cells. *J Leukoc Biol* 2018;104:883-93.
 49. Olingy CE, Dinh HQ, Hedrick CC. Monocyte heterogeneity and functions in cancer. *J Leukoc Biol* 2019;106:309-22.
 50. Wu K, Lin K, Li X, et al. Redefining Tumor-Associated Macrophage Subpopulations and Functions in the Tumor Microenvironment. *Front Immunol* 2020;11:1731.
 51. Park SM, Chen CJ, Verdon DJ, et al. Proliferating macrophages in human tumours show characteristics of monocytes responding to myelopoietic growth factors. *Front Immunol* 2024;15:1412076.
 52. Prinz M, Jung S, Priller J. Microglia Biology: One Century of Evolving Concepts. *Cell* 2019;179:292-311.
 53. Worbs T, Hammerschmidt SI, Förster R. Dendritic

cell migration in health and disease. *Nat Rev Immunol* 2017;17:30-48.
54. Zhang J, Xu X, Shi M, et al. CD13(hi) Neutrophil-like

myeloid-derived suppressor cells exert immune suppression through Arginase 1 expression in pancreatic ductal adenocarcinoma. *Oncoimmunology* 2017;6:e1258504.

Cite this article as: Guan Y, Luan Y, Zhao S, Li M, Girolamo F, Palmer JD, Guan Q. Single-cell RNA sequencing for characterizing the immune communication and iron metabolism roles in CD31⁺ glioma cells. *Transl Cancer Res* 2025;14(4):2421-2439. doi: 10.21037/tcr-2025-377